Published online May 11, 2004

2556–2565 *Nucleic Acids Research, 2004, Vol. 32, No. 8*
DOI: 10.1093/nar/gkh578

Preferential binding to branched DNA strands and strand-annealing activity of the human Rad51B, Rad51C, Rad51D and Xrcc2 protein complex

Hiroshi Yokoyama[1,2], Naoyuki Sarai[1,2], Wataru Kagawa[1], Rima Enomoto[1], Takehiko Shibata[3,4], Hitoshi Kurumizaka[1,4,5,*] and Shigeyuki Yokoyama[1,2,6]

[1]RIKEN Genomic Sciences Center, 1-7-22 Suehiro-cho, Tsurumi, Yokohama 230-0045, Japan, [2]Department of Biophysics and Biochemistry, Graduate School of Science, University of Tokyo, 7-3-1 Hongo, Bunkyo-ku, Tokyo 113-0033, Japan, [3]Cellular and Molecular Biology Laboratory, RIKEN, 2-1 Hirosawa, Wako-shi, Saitama 351-0198, Japan, [4]Core Research for Evolutional Science and Technology (CREST), Japan Science and Technology Corporation, 1637 Yana, Kisarazu, Chiba 292-0812, Japan, [5]Waseda University School of Science and Engineering, 3-4-1 Okubo, Shinjuku-ku, Tokyo 169-8555, Japan and [6]RIKEN Harima Institute at Spring-8, 1-1-1 Kohto, Mikazuki-cho, Sayo, Hyogo 679-5148, Japan

Received March 8, 2004; Revised and Accepted April 12, 2004

ABSTRACT

The Rad51B, Rad51C, Rad51D and Xrcc2 proteins are Rad51 paralogs, and form a complex (BCDX2 complex) in mammalian cells. Mutant cells defective in any one of the Rad51-paralog genes exhibit spontaneous genomic instability and extreme sensitivity to DNA-damaging agents, due to inefficient recombinational repair. Therefore, the Rad51 paralogs play important roles in the maintenance of genomic integrity through recombinational repair. In the present study, we examined the DNA-binding preference of the human BCDX2 complex. Competitive DNA-binding assays using seven types of DNA substrates, single-stranded DNA (ssDNA), double-stranded DNA, 5′- and 3′-tailed duplexes, nicked duplex DNA, Y-shaped DNA and a synthetic Holliday junction, revealed that the BCDX2 complex preferentially bound to the two DNA substrates with branched structures (the Y-shaped DNA and the synthetic Holliday junction). Furthermore, the BCDX2 complex catalyzed the strand-annealing reaction between a long linear ssDNA (1.2 kb in length) and its complementary circular ssDNA. These properties of the BCDX2 complex may be important for its roles in the maintenance of chromosomal integrity.

INTRODUCTION

Chromosomes are continuously subjected to attacks by endogenous and exogenous mutagens, which cause various forms of DNA damage. A double strand break (DSB) within a chromosome is one of the most severe DNA lesions, and is caused by ionizing radiation, oxygen free-radicals derived from normal metabolism, DNA crosslinking reagents and DNA replication failure. DSBs potentially lead to chromosomal aberrations and tumorigenesis (1–4). To prevent the accumulation of DSBs, cells employ homologous recombinational repair (HRR), an accurate DSB repair pathway that utilizes a homologous region of the undamaged chromosome as the template, and this is free of base substitutions, deletions and insertions (5). Therefore, recombinational repair is important in maintaining the chromosomal integrity.

The bacterial RecA protein plays central roles in HRR. RecA catalyzes the strand invasion and strand-exchange reactions in the early stages of HRR (6–9). The eukaryotic Rad51 protein, a structural and functional homolog of RecA, shares similar recombinational activities to those of RecA (10–14). In vertebrates, five Rad51 paralogs, Rad51B/REC2/Rad51L1 (15–17), Rad51C/Rad51L2 (18), Rad51D/Rad51L3 (17,19), Xrcc2 (20,21) and Xrcc3 (21,22), which share ~20% amino acid identity with the human Rad51 protein, have been identified. Mutant cells defective in any one of the Rad51-paralog genes exhibit extreme sensitivities to DNA cross-linking agents, such as cisplatin and mitomycin C, and show spontaneous chromosomal aberrations (21–27). Moreover, the nuclear focus formation of Rad51 was significantly attenuated in these mutant cells, suggesting that the Rad51 paralogs may support Rad51-mediated recombination (25–28). These

*To whom correspondence should be addressed. Tel: + 81 3 5286 8189; Fax: + 81 3 5292 9211; Email: kurumizaka@waseda.jp
Correspondence may also be addressed to Shigeyuki Yokoyama. Tel: +81 45 503 9196; Fax: +81 45 503 9195; Email: yokoyama@biochem.s.u-tokyo.ac.jp
Present address:
Hiroshi Yokoyama, National Agriculture and Bio-oriental Research Organization, National Institute of Livestock and Grassland Science, 2 Ikenodai, Tsukuba, Ibaraki 305-0901, Japan

The authors wish it to be known that, in their opinion, the first two authors should be regarded as joint First Authors

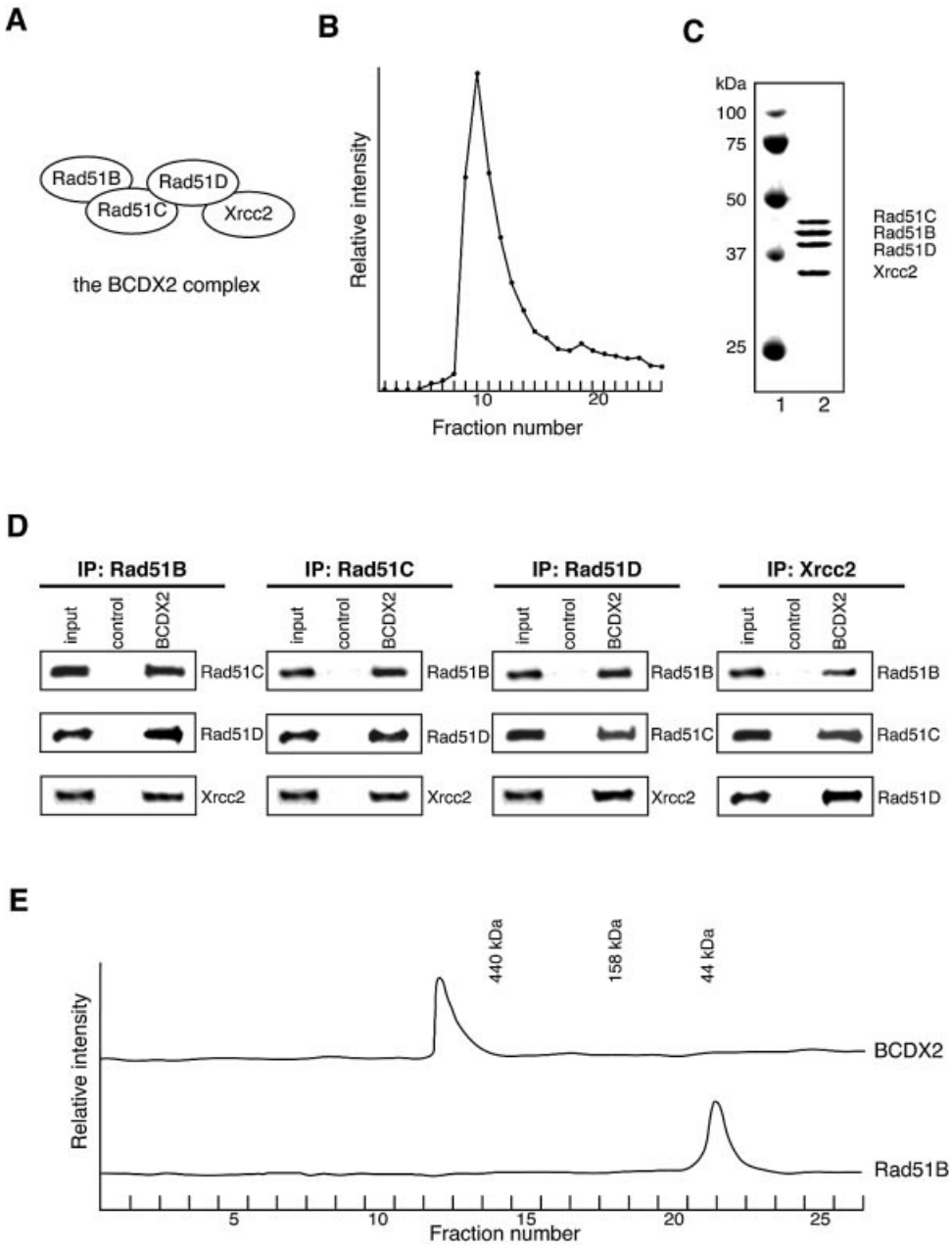

Figure 1. Purification of the BCDX2 complex. (**A**) Schematic representation of protein interactions within the BCDX2 complex. These protein interactions were previously identified by two-hybrid and biochemical analyses. (**B**) Elution profile of the Rad51B, Rad51C, Rad51D and Xrcc2 proteins in DEAE column chromatography. (**C**) The peak fraction (2 μg, lane 2) from the DEAE column was analyzed by 12% SDS–PAGE, and was stained with Coomassie Brilliant Blue. Lane 1 shows the molecular mass markers. (**D**) Immunoprecipitation (IP) experiments of the co-purified Rad51B, Rad51C, Rad51D and Xrcc2 proteins. The co-purified proteins were captured using anti-Rad51B, Rad51C, Rad51D or Xrcc2 antibody-conjugated beads, and the precipitates were analyzed by immunoblotting. As negative-control experiments, the co-purified proteins were incubated with normal IgG-conjugated beads. (**E**) Elution profiles of the co-purified Rad51B, Rad51C, Rad51D, and Xrcc2 proteins (upper) and the Rad51B protein (lower) in Superdex 200 HR gel filtration column chromatography.

findings indicate that the Rad51 paralogs are important to maintain chromosomal integrity and function in the early stages of HRR.

Analyses employing a two-hybrid system and immunoprecipitation experiments indicated that the Rad51 paralogs form two distinct complexes in human cells; one complex consists of Rad51B, Rad51C, Rad51D and Xrcc2 (BCDX2), and the other complex consists of Rad51C and Xrcc3 (Fig. 1A) (29–36). In the BCDX2 complex, Rad51C binds to Rad51B and Rad51D, and Rad51D binds to Xrcc2 (Fig. 1A) (36,37). In addition, two sub-complexes (Rad51B·Rad51C and Rad51D·Xrcc2) were purified as recombinant proteins (33,38–41). The Rad51B·Rad51C and Rad51D·Xrcc2 sub-complexes bound to single-stranded DNA (ssDNA) and double-stranded DNA (dsDNA), and hydrolyzed ATP (38–40). The Rad51B·Rad51C sub-complex reportedly supports the strand-exchange reaction mediated by the Rad51 and RPA proteins (40). Furthermore, two forms of Rad51C, alone and in the Rad51C·Xrcc3 complex, have been purified, and they exhibited the homologous pairing activities (29,38). In

addition, it was reported that the BCDX2 complex specifically binds to nicks in a dsDNA molecule (30).

Revealing the DNA-binding preferences of recombination proteins is the key to understanding their roles in HRR. We previously demonstrated that Rad51B preferentially bound to a synthetic Holliday junction over other types of DNA substrates (42), suggesting that the BCDX2 complex may be involved in not only the early stages but also the late stages of HRR. Recently, Rad51C was shown to be required for Holliday junction processing (43), and the involvement of Rad51 paralogs in the late stages of HRR is a current topic of interest in the field of DNA recombination. In the present study, we purified the recombinant human BCDX2 complex, and examined its DNA-binding preferences using various types of DNA substrates with defined structures. We also investigated the biochemical activities of the BCDX2 complex. We found two interesting properties of the BCDX2 complex: preferential binding to branched DNA strands, including the Holliday junction, and strand-annealing activity between plasmid-sized ssDNAs. These findings should help to clarify the roles of the BCDX2 complex in the maintenance of chromosomal integrity.

MATERIALS AND METHODS

Protein purification

To obtain the recombinant human BCDX2 complex, the Rad51B·Rad51C and Rad51D·Xrcc2 proteins were separately expressed in the *Escherichia coli* JM109(DE3) strain, as His_6-tagged proteins at their N-terminal ends, using the pET-15b vector (Novagen). Both strains producing the Rad51B·Rad51C and Rad51D·Xrcc2 proteins also carried another plasmid that expressed the minor tRNAs [Codon(+)RIL, Novagen]. After the bacteria producing the Rad51B·Rad51C and Rad51D·Xrcc2 proteins were mixed, the cells were harvested. The cells were disrupted by sonication in a buffer (pH 8.5) containing 20 mM Tris–HCl, 0.5 M NaCl, 0.02% Triton X-100, 2 mM 2-mercaptoethanol (2ME) and 10% glycerol. The cell debris was removed by centrifugation for 20 min at 30 000 *g*, and the lysate was mixed gently with 4 ml of Ni-NTA (Invitrogen) beads by the batch method at 4°C for 1 h. The beads with the bound His_6-Rad51B, His_6-Rad51C, His_6-Rad51D and His_6-Xrcc2 proteins were then packed into an Econo-column (Bio-Rad), and were washed with 15 column volumes (CV) of a buffer (pH 8.5) containing 20 mM Tris–HCl, 0.5 M NaCl, 0.02% Triton X-100, 2 mM 2ME, 10% glycerol and 30 mM imidazole, at a flow rate of ~0.3 ml/min. The beads were further washed with 10 CV of a buffer (pH 8.5) containing 20 mM Tris–HCl, 0.02% Triton X-100, 2 mM 2ME, 10% glycerol and 30 mM imidazole. The His_6-Rad51B, His_6-Rad51C, His_6-Rad51D and His_6-Xrcc2 proteins were eluted by a linear gradient of 30–400 mM imidazole in a buffer (pH 8.5) containing 20 mM Tris–HCl, 0.02% Triton X-100, 2 mM 2ME and 10% glycerol, and were dialyzed against a dialysis buffer (pH 8.1) containing 20 mM Tris–HCl, 0.02% Triton X-100, 2 mM 2ME, 0.1 mM ethylenediaminetetraacetate (EDTA) and 10% glycerol. The dialyzed proteins were applied to a 4 ml DEAE column (diethylaminoethyl cellulose, Whatman) equilibrated with the dialysis buffer. After washing with 10 CV of the dialysis buffer, the His_6-Rad51B, His_6-Rad51C, His_6-Rad51D and His_6-Xrcc2 proteins were eluted by a linear gradient of 0–1.5 M NaCl in the dialysis buffer. The proteins eluted from the DEAE column were further analyzed by Superdex 200 HR gel filtration chromatography (Amersham Biosciences) in the dialysis buffer, at a flow rate of 0.2 ml/min. The proteins eluted from the DEAE column were also analyzed by gel filtration column chromatography in dialysis buffer supplemented with 0.15 M NaCl, and a similar result was obtained (data not shown).

The human Rad51, Rad51B and Rad52 proteins and the *E.coli* RecA protein were purified as described (42,44–46). The concentrations of the purified proteins were determined with a Bio-Rad protein assay kit, using bovine serum albumin (BSA) as the standard. The concentration of the BCDX2 complex is expressed as the heterotetramer.

Oligonucleotides

The synthetic Holliday junction was composed of four 49mer single-stranded oligonucleotides, 1, 2, 3 and 4, with the sequences 5′-ATCGA TGTCT CTAGA CAGCT GCTCA GGATT GATCT GTAAT GGCCT GGGA-3′, 5′-GTCCC AGGCC ATTAC AGATC AATCC TGAGC ATGTT TACCA AGCGC ATTG-3′, 5′-TGATC ACTTG CTAGC GTCGC AATCC TGAGC AGCTG TCTAG AGACA TCGA-3′ and 5′-CCAAT GCGCT TGGTA AACAT GCTCA GGATT GCGAC GCTAG CAAGT GATC-3′, respectively. The resulting junction contained a 12 bp homologous region at the center, and the four 5′ ends each had one base overhangs. The Y-shaped DNA, which was produced by annealing oligonucleotides 1 and 2, was composed of a 30 bp duplex region, and two 18 and 19 bp heterologous single strands. The double-stranded oligonucleotide was produced by annealing oligonucleotide 2 with its complementary oligonucleotide. The 5′-tailed duplex was produced by annealing oligonucleotide 2 and the 25mer oligonucleotide 5, with the sequence 5′-CAATG CGCTT GGTAA ACATG CTCAG-3′, and was composed of a 25 bp duplex region and a 24 bp single strand with a 5′-end. The 3′-tailed duplex was produced by annealing oligonucleotide 2 and the 24mer oligonucleotide 6, with the sequence 5′-GATTG ATCTG TAATG GCCTG GGAC-3′, and was composed of a 24 bp duplex region and a 25 bp single strand with a 3′-end. The nicked duplex was produced by annealing oligonucleotides 2, 5 and 6. In the DNA-binding assays, the 5′-end of oligonucleotide 2 was labeled with T4 polynucleotide kinase (New England Biolabs) in the presence of [γ-^{32}P]ATP. All of the oligonucleotides were purified by HPLC, and the DNA concentrations are expressed in moles of nucleotides.

Immunoprecipitation assay

The BCDX2 complex (2 μg) was incubated with 10 μl of anti-Rad51B, Rad51C, Rad51D or Xrcc2 antibody-conjugated rProtein A Sepharose Fast Flow (Amersham Biosciences), in a binding buffer containing 20 mM phosphate (pH 7.7), 150 mM NaCl, 2 mM 2ME, 0.05% Triton X-100, 0.1 mM EDTA and 10% glycerol, at 4°C for 1 h. The beads were washed three times with 500 μl of phosphate buffered saline containing 1% NP-40, and were eluted by the addition of 2× SDS (sodium dodecyl sulfate) gel-loading buffer [100 mM Tris–HCl (pH 6.8), 200 mM dithiothreitol (DTT), 4% SDS, 0.2% bromophenol blue and 20% glycerol]. The eluted fractions

were separated by 15–25% gradient SDS–polyacrylamide gel electrophoresis (PAGE), and were blotted onto a polyvinylidene fluoride membrane. The proteins transferred on the membrane were analyzed by immunoblotting. The rabbit anti-Rad51B and Rad51D antibodies were prepared in this study, and the rabbit anti-Rad51C antibody was described previously (35). Goat anti-Xrcc2 antibody (N-20) was purchased from Santa Cruz Biotechnology. These anti-Rad51 paralog antibodies did not cross-react with the other Rad51 paralog proteins (data not shown).

ATPase assay

The ATPase activities of the BCDX2 complex were analyzed by the release of ^{32}Pi from [γ-^{32}P]ATP. The reaction mixtures contained 25 mM bis-Trispropane–HCl (pH 7.5), 1 mM $MgCl_2$, 1 mM ATP, 50 nCi [γ-^{32}P]ATP, 50 mM NaCl, 2 mM DTT, 15% glycerol, 100 μg/ml BSA, 0.05% Triton X-100, 75 μM M13mp19 ssDNA and 1 μM BCDX2 complex. After incubations at 37°C for the indicated times, the reactions were stopped by adding one-half volume of 0.5 M EDTA. The samples were separated by thin layer chromatography on polyethyleneimine-cellulose (Sigma) in a 0.5 M LiCl and 1.0 M formic acid solution, and were quantified by a Fuji BAS2500 image analyzer.

Single-stranded and double-stranded DNA binding assays

pGsat4 is derived from the pGEM-T Easy vector (Promega), and contains the human α-satellite sequence at the TA-cloning site of that vector. pGsat4 ssDNA (20 μM) or ϕX174 dsDNA (10 μM) was mixed with the indicated amounts of the BCDX2 complex in a 10 μl reaction mixture, containing 25 mM bis-Trispropane–HCl (pH 7.5), 1 mM ATP, 2 mM DTT, 100 μg/ml BSA, 2 mM $MgCl_2$, 15% glycerol, 50 mM NaCl and 0.05% Triton X-100. The reaction mixtures were incubated at 30°C for 10 min, and were analyzed by 1% agarose gel electrophoresis for 4 h at 3 V/cm in 0.5× TBE buffer (45 mM Tris, 45 mM boric acid and 1 mM EDTA, pH 8.3). The bands were stained with ethidium bromide.

Holliday-junction binding and competitive DNA-binding assays

The indicated amounts of the BCDX2 complex were incubated at 30°C for 10 min in the presence of 0.33 μM substrates in the indicated combinations. The reaction mixtures contained 25 mM bis-Trispropane–HCl (pH 7.5), 1 mM ATP, 2 mM DTT, 100 μg/ml BSA, 2 mM $MgCl_2$, 15% glycerol, 50 mM NaCl and 0.05% Triton X-100. The products were analyzed by 10% native PAGE in 0.5× TBE buffer, and were visualized and quantified using the Fuji BAS2500 image analyzer.

DNA substrates for the strand-annealing assay

Circular ssDNA (pGsat4, 3216 bases) was prepared using the R408 Helper Phage (Promega), as described (44). An additional gel extraction purification was performed by fractionation on a 1% agarose gel in TAE buffer (40 mM Tris-acetate and 1 mM EDTA). To locate the fractionated DNA, only the side portions of the agarose gel were stained with ethidium bromide. This was done to avoid irreversible denaturation of the amplified DNA substrates by ethidium-bromide staining and UV irradiation. The unstained portion of the gel containing the circular ssDNA was excised, and the ssDNA was purified with a Gel Extraction Kit (Qiagen).

The complementary linear ssDNA substrate (1152 bases) was prepared by amplifying a region of pGsat4 by polymerase chain reaction (PCR), followed by the exonucleolytic digestion of one of the DNA strands with lambda exonuclease. First, a DNA fragment was amplified from pGsat4 by PCR using two primers, a 25mer forward primer (AGTAT ATATG AGTAA ACTTG GTCTG) and a 25mer reverse primer (CTCAT TTTTT AACCA ATAGG CCGAA). The 5′-end of the reverse primer was phosphorylated. The PCR reaction mixture (200 μl) contained 120 mM Tris–HCl (pH 8.0), 10 mM KCl, 6 mM ammonium sulfate, 0.1% Triton X-100, 10 μg/ml BSA, 200 μM each dNTP (dATP, dTTP, dGTP and dCTP), 100 ng pGsat4, 0.6 μM each of the forward and reverse primers, 2.5 mM $MgCl_2$ and 10 U KOD Dash DNA polymerase (TOYOBO). The reaction program was as follows: one cycle at 94°C for 1 min, 25 cycles of 94°C for

A

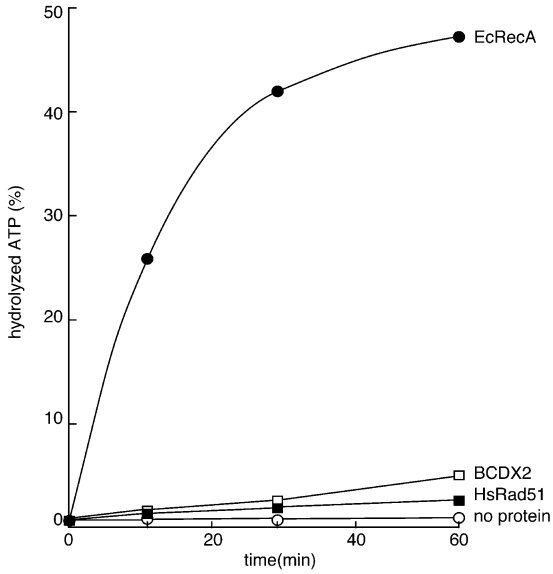

B

	K_m	V_{max}	k_{cat}
	μM	μM•min^{-1}	min^{-1}
BCDX2	130 ± 19	0.88 ± 0.12	0.88

Figure 2. ATPase activity of the BCDX2 complex. (**A**) Comparison of the ATPase activities among the BCDX2 complex, HsRad51 and EcRecA proteins. The ATPase activities of the three proteins were measured in the presence of 1 mM ATP and 75 μM ssDNA, and the percentages of hydrolyzed ATP at the indicated time points are presented. The open squares and the open circles indicate the experiments with the BCDX2 complex and without protein, respectively, and the closed squares and the closed circles indicate the experiments with HsRad51 and EcRecA, respectively. (**B**) Table of K_m, V_{max} and k_{cat} values for the ATPase activity of the BCDX2 complex in the presence of ssDNA.

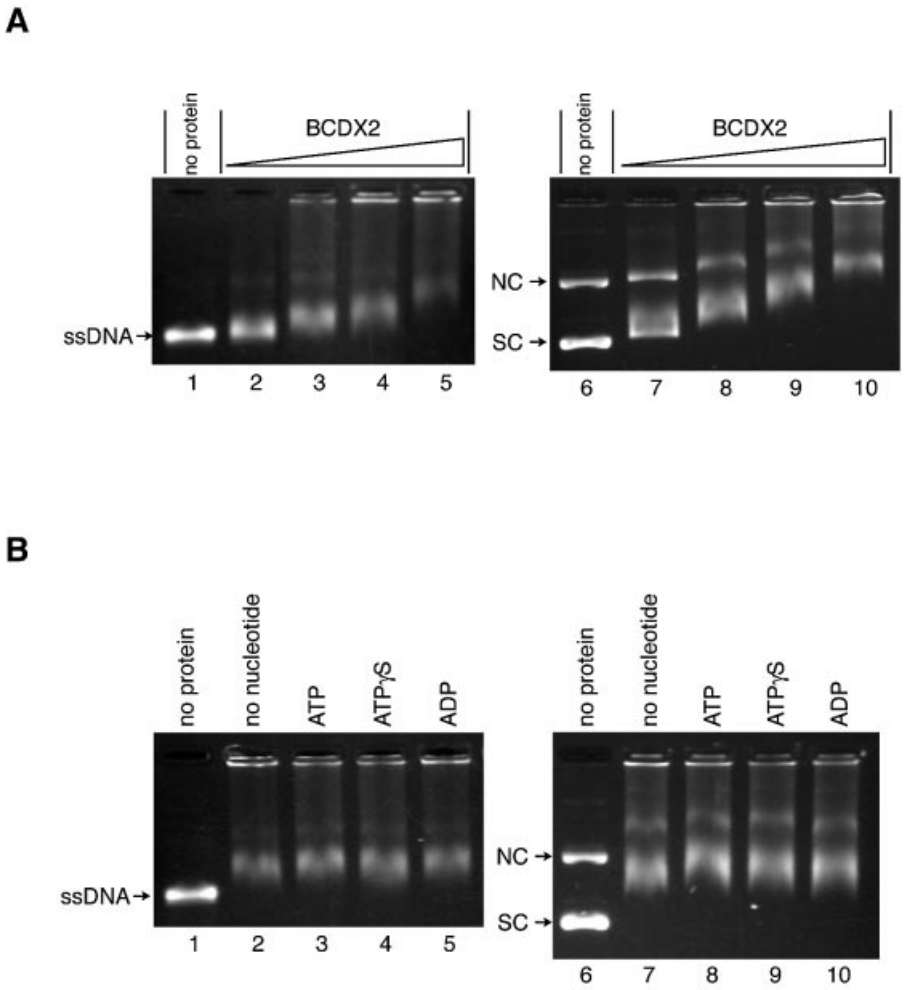

Figure 3. DNA-binding activities of the BCDX2 complex. (**A**) ssDNA and dsDNA binding by the BCDX2 complex. pGsat4 ssDNA (20 μM, lanes 1–5) or ϕX174 superhelical dsDNA (10 μM, lanes 6–10) was incubated with the BCDX2 complex at 30°C for 10 min. The concentrations of the BCDX2 complex used in the DNA-binding experiments were 0.12 μM (lanes 2 and 7), 0.35 μM (lanes 3 and 8), 0.69 μM (lanes 4 and 9) and 1.2 μM (lanes 5 and 10). The samples were analyzed by 1% agarose gel electrophoresis in 0.5× TBE buffer, and were stained with ethidium bromide (A and B). NC and SC indicate nicked circular and superhelical dsDNA, respectively (A and B). Lanes 1 and 5 indicate the negative control experiments without protein. (**B**) Nucleotide co-factor requirements for ssDNA and dsDNA binding. pGsat4 ssDNA (20 μM, lanes 1–5) or ϕX174 superhelical dsDNA (10 μM, lanes 6–10) was incubated with the BCDX2 complex (0.69 μM) at 30°C for 10 min in the presence of 1 mM ATP (lanes 3 and 8), 1 mM ATPγS (lanes 4 and 9) or 1 mM ADP (lanes 5 and 10). Lanes 1 and 6 indicate the negative control experiments without protein, and lanes 2 and 7 indicate the negative control experiments without nucleotide co-factor.

30 s, 40°C for 2 s and 74°C for 90 s, and a final cycle at 74°C for 5 min. The PCR product was fractionated on a 1% agarose gel in TAE buffer, and was purified as described above. Second, the strand with the phosphorylated 5′-end was digested with lambda exonuclease (New England Biolabs) to produce the linear ssDNA. The preferred substrate of lambda exonuclease is 5′-phosphorylated dsDNA, although it will also degrade single-stranded and non-phosphorylated substrates at a greatly reduced rate. The reaction mixture, containing 67 mM glycine-KOH (pH 9.4), 2.5 mM $MgCl_2$, 50 μg/ml BSA, 30 μM DNA fragment and 100 U/ml lambda exonuclease, was incubated at 37°C for 2 h. When the DNA concentration was higher than 30 μM, the digestion by the lambda exonuclease was incomplete. In addition, when the incubation time of the nuclease digestion was over 2 h, the yield of the linear ssDNA was extremely low, due to degradation of the non-phosphorylated ssDNA by the lambda exonuclease. Therefore, the linear ssDNA produced by the nuclease digestion was immediately purified after the 2 h incubation, using a Nucleotide Removal Kit (Qiagen). The 5′-end of the linear ssDNA was labeled with T4 polynucleotide kinase (New England Biolabs) in the presence of [γ-^{32}P]ATP.

Strand-annealing assay

The indicated amounts of the BCDX2 complex were incubated with the ^{32}P-labeled linear ssDNA (1.2 kb, 35 nM) at 30°C for 5 min. The reaction mixtures contained 25 mM bis-Trispropane–HCl (pH 7.5), 2 mM DTT, 100 μg/ml BSA, 2 mM $MgCl_2$, 15% glycerol, 0.5 mM ammonium sulfate and 0.05% Triton X-100. The strand-annealing reactions were started by the addition of the circular ssDNA (3.2 kb, 400 nM) and 1 mM ATP. After an incubation at 37°C for 10 min, the reactions were stopped by the addition of the unlabeled linear ssDNA (700 nM) and 0.5% SDS, and the products were deproteinized with Proteinase K. The samples were analyzed by 0.8%

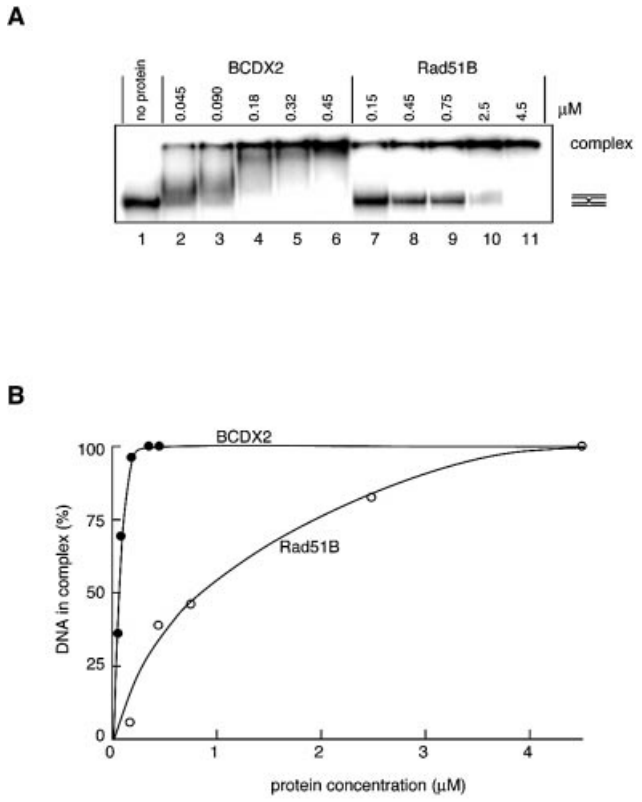

Figure 4. Holliday junction binding by the BCDX2 complex. (**A**) The ^{32}P-labeled synthetic Holliday junction (0.33 μM) was incubated with the indicated amounts of the BCDX2 complex (lanes 2–6) or the Rad51B protein (lanes 7–11) at 30°C for 10 min. The samples were separated by electrophoresis on a 10% non-denaturing polyacrylamide gel in 0.5× TBE buffer, and were analyzed by the BAS2500 image analyzer. (**B**) Graphic representation of the amounts of the synthetic Holliday junction incorporated into the complex shown in (A). The closed and open circles indicate the experiments with the BCDX2 complex and Rad51B, respectively.

agarose gel electrophoresis in TAE buffer, and were visualized and quantified by the Fuji BAS2500 image analyzer.

RESULTS

Purification of the BCDX2 complex

To reconstitute the human BCDX2 complex (161 kDa), the Rad51B·Rad51C and Rad51D·Xrcc2 proteins were separately co-expressed in *E.coli* as hexahistidine tagged fusion proteins. After mixing the bacteria expressing the Rad51B·Rad51C and Rad51D·Xrcc2 proteins, the cells were disrupted by sonication. The four Rad51-paralog proteins were detected in the soluble fraction, and were co-purified by Ni-NTA column chromatography, followed by DEAE column chromatography. The four Rad51-paralog proteins were co-eluted from the DEAE column as a single sharp peak (Fig. 1B), implying that they formed a stable complex. The co-purified Rad51B, Rad51C, Rad51D and Xrcc2 proteins were fractionated by SDS–PAGE, and the apparent stoichiometry was nearly 1:1:1:1 (Fig. 1C, lane 2).

Immunoprecipitation and gel filtration analyses were then carried out to confirm that the co-purified proteins were actually forming a stable complex. When the co-purified proteins were captured with the anti-Rad51B, Rad51C, Rad51D or Xrcc2 antibody-conjugated beads, the other three proteins were co-precipitated (Fig. 1D). In the Superdex 200 HR gel filtration column chromatography, the co-purified proteins eluted near the void volume, corresponding to >600 kDa (Fig. 1E, upper), and no monomeric forms of the Rad51 paralogs were detected. As a control experiment, Rad51B (40 kDa) alone was analyzed by gel filtration column chromatography, and was eluted in fractions corresponding to the monomeric form (Fig. 1E, lower). Therefore, these results indicated that the co-purified proteins formed the BCDX2 complex, and the reconstituted BCDX2 complex was self-associated *in vitro*.

ATPase activities of the BCDX2 complex

The Rad51B (15–17), Rad51C (18), Rad51D (17,19) and Xrcc2 (20,21) proteins have the Walker A-type motif, which is known to bind and hydrolyze ATP. A previous study on the BCDX2 complex prepared from insect cells revealed that it hydrolyzes ATP in the presence of ssDNA (30). To further characterize the ATPase activity of the BCDX2 complex, we compared it with those of the human Rad51 (HsRad51) and *E.coli* RecA (EcRecA) proteins in the presence of ssDNA. As shown in Figure 2A, the ATPase activity of the BCDX2 complex was slightly higher than that of HsRad51, and was much lower than that of EcRecA. To more quantitatively analyze the ATPase activity of the BCDX2 complex, its K_m, V_{max} and k_{cat} values in the presence of ssDNA were determined, using the Michaelis–Menten equation (Fig. 2B). The k_{cat} value, which indicates the turnover rate, for the BCDX2 complex (0.88 min^{-1}) is ~4-fold higher and ~32-fold lower than those values previously reported for HsRad51 (0.21 min^{-1}) (13,47) and EcRecA (28 min^{-1}) (48–53), respectively.

Single-stranded DNA and double-stranded DNA-binding activities of the BCDX2 complex

We next examined the DNA-binding properties of the BCDX2 complex. pGsat4 circular ssDNA (3.2 kb) and ϕX174 superhelical dsDNA (5.4 kb) were used for the ssDNA- and dsDNA-binding assays, respectively. As shown in Figure 3A, the BCDX2 complex bound to both ssDNA (lanes 2–5) and dsDNA (lanes 7–10). Neither ATP, ADP nor ATPγS influenced the ssDNA- and dsDNA-binding of the BCDX2 complex (Fig. 3B).

Holliday junction-binding activity of the BCDX2 complex

We previously reported that Rad51B preferentially binds to a synthetic Holliday junction (42). Therefore, we next tested the synthetic Holliday-junction binding of the BCDX2 complex. The BCDX2 complex also bound to the synthetic Holliday junction, and its affinity to the Holliday-junction DNA was significantly higher than that of Rad51B (Fig. 4). The concentration of the BCDX2 complex (65 nM) required for 50% Holliday junction binding was ~13-fold lower than that of Rad51B (870 nM).

Preferential binding of the BCDX2 complex to branched DNA strands

Since the Holliday junction-binding activity of the BCDX2 complex was found, the binding preference of the complex to

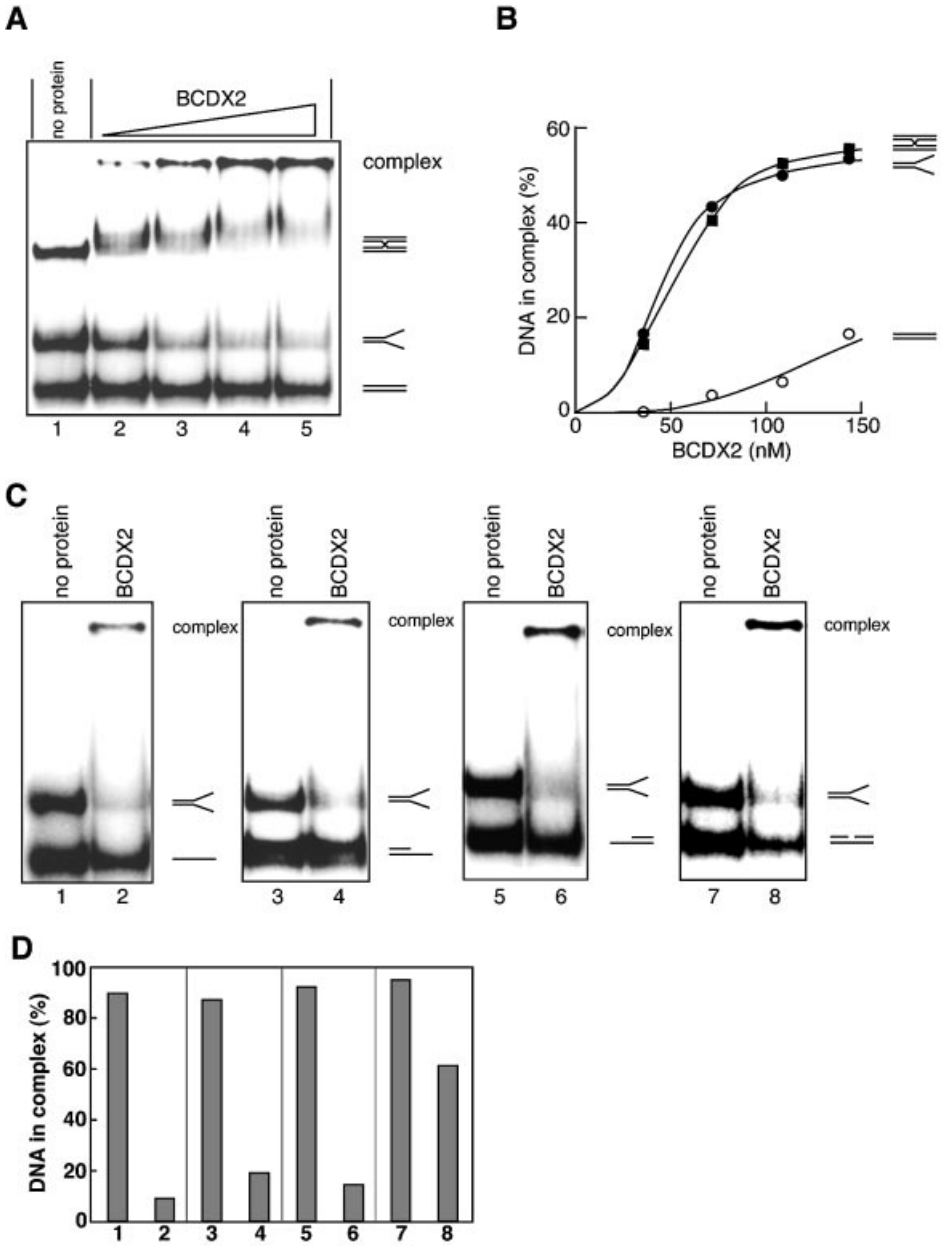

Figure 5. Preferential binding of the BCDX2 complex to branched DNA strands. (**A**) Increasing amounts of the BCDX2 complex were incubated with the DNA mixture, containing the three ^{32}P-labeled DNA substrates (0.33 μM each), the synthetic Holliday junction, the Y-shaped DNA and the double-stranded oligonucleotide, at 30°C for 10 min. The samples were separated by electrophoresis on a 10% non-denaturing polyacrylamide gel in 0.5× TBE buffer, and were analyzed by the BAS2500 image analyzer. The concentrations of the BCDX2 complex used in the DNA-binding experiments were 36, 72, 110 and 140 nM (lanes 2–5). (**B**) Graphic representation of the amounts of each DNA incorporated into the complex shown in (A). The squares, closed circles and open circles indicate the synthetic Holliday junction, the Y-shaped DNA, and the double-stranded oligonucleotide, respectively. (**C**) The Y-shaped DNA (0.33 μM) was separately mixed with 0.33 μM of the four DNA substrates, a single-stranded oligonucleotide (lanes 1 and 2), a 5′-tailed duplex (lanes 3 and 4), a 3′-tailed duplex (lanes 5 and 6) or a nicked duplex (lanes 7 and 8), and was incubated with the BCDX2 complex (110 nM) at 30°C for 10 min. The samples were separated by electrophoresis on a 10% non-denaturing polyacrylamide gel in 0.5× TBE buffer, and were analyzed by the BAS2500 image analyzer. Lanes 1, 3, 5 and 7 indicate negative control experiments without protein. (**D**) Graphic representation of the amounts of each DNA incorporated into the complex shown in (C). Lanes 1 and 2 indicate the competition experiment with the Y-shaped DNA and the single-stranded oligonucleotide. Lanes 3 and 4 indicate the competition experiment with the Y-shaped DNA and the 5′-tailed duplex. Lanes 5 and 6 indicate the competition experiment with the Y-shaped DNA and the 3′-tailed duplex. Lanes 7 and 8 indicate the competition experiment with the Y-shaped DNA and the nicked duplex. Lanes 1, 3, 5 and 7 indicate the amounts of the Y-shaped DNA incorporated into the complex. Lanes 2, 3, 4, 6 and 8 indicate the amount of the single-stranded oligonucleotide, the 5′-tailed duplex, the 3′-tailed duplex, and the nicked duplex incorporated into the complex, respectively.

various types of DNA substrates was examined. Three DNA substrates, the synthetic Holliday junction, a Y-shaped DNA and a double-stranded oligonucleotide, were mixed with the BCDX2 complex. The DNA–protein complexes were subsequently fractionated by native PAGE. Interestingly, the BCDX2 complex preferentially bound to the two branched DNA substrates, the synthetic Holliday junction and the Y-shaped DNA (Fig. 5A and B). We next tested the

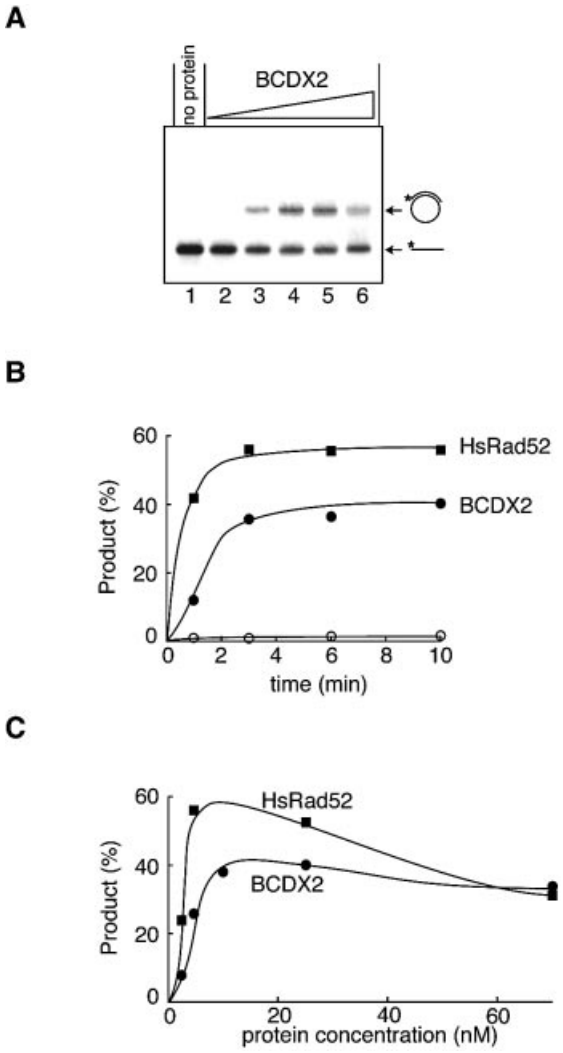

Figure 6. Strand-annealing activities of the BCDX2 complex. (**A**) Increasing amounts of the BCDX2 complex were incubated with the ^{32}P-labeled linear ssDNA (1.2 kb, 35 nM) at 30°C for 5 min, and the strand-annealing reactions were started by the addition of the circular ssDNA (3.2 kb, 400 nM) and 1 mM ATP. After an incubation at 37°C for 10 min, the reactions were stopped by the addition of unlabeled linear ssDNA and 0.5% SDS, and the products were deproteinized with Proteinase K. The samples were analyzed by 0.8% agarose gel electrophoresis in TAE buffer, and were visualized by the BAS2500 image analyzer. The concentrations of the BCDX2 complex used in the strand-annealing experiments were 2, 4, 10, 25 and 70 nM (lanes 2–6). Lane 1 indicates a negative control experiment without protein. (**B** and **C**) Comparison of the strand-annealing activities between the BCDX2 complex and HsRad52, as functions of time (B) and protein concentration (C). (B) The closed circles and squares indicate the reactions of the BCDX2 complex (25 nM) and HsRad52 (25 nM), respectively, and the open circles indicate the negative control experiments without protein. (C) The circles and squares indicate the experiments with the increasing amounts of the BCDX2 complex and HsRad52, respectively.

DNA-binding preference of the BCDX2 complex with four other DNA substrates, a single-stranded oligonucleotide, a 5′-tailed duplex, a 3′-tailed duplex and a nicked duplex. These four unbranched DNA substrates were separately mixed with the Y-shaped DNA, and were incubated with the BCDX2 complex. As shown in Figure 5C and D, the BCDX2 complex preferentially bound to the Y-shaped DNA, rather than the four DNA substrates lacking branched structures. Therefore, we conclude that the BCDX2 complex preferentially binds to branched DNA strands. The BCDX2 complex reportedly binds to nicked linear dsDNA more strongly than linear dsDNA (30). Actually, ~60% of the nicked duplex was bound to the BCDX2 complex in the presence of the Y-shaped DNA (Fig. 5D, lane 8). On the other hand, the amounts of the single-stranded oligonucleotide, the 5′-tailed duplex, and the 3′-tailed duplex bound to the BCDX2 complex were only 9.3, 19.8 and 15.0%, respectively (Fig. 5D, lanes 2, 4 and 6). Therefore, the BCDX2 complex also preferred the nicked duplex DNA.

Strand-annealing activities of the BCDX2 complex

The DNA-binding preference of the BCDX2 complex led us to predict that the complex binds to Y-shaped DNA *in vivo*, and then moves the branch of the Y-shaped structure by the strand-annealing reaction. Therefore, we examined the strand-annealing activity of the BCDX2 complex, using long ssDNA substrates (1.2 kb) prepared by digesting the dsDNA fragment with lambda exonuclease. As shown in Figure 6A, the BCDX2 complex catalyzed the strand-annealing reaction between the 1.2 kb ssDNA and its complementary circular ssDNA (3.2 kb). No spontaneous reaction was detected in the strand-annealing assay, probably due to the secondary structure in the DNA strands (Fig. 6A, lane 1). To further characterize the strand-annealing activity of the BCDX2 complex, we compared its activity with that of the human Rad52 protein (HsRad52), which is a well known annealing enzyme in HRR (Fig. 6B and C) (54–56). The BCDX2 complex exhibited approximately two-thirds of the strand-annealing activity displayed HsRad52, based on a comparison of their peak points.

DISCUSSION

In the present study, we have found two properties of the BCDX2 complex that could help to clarify its role in HRR. One is the preferential binding to branched DNA strands, and the other is the strand-annealing activity between plasmid-sized ssDNAs. The BCDX2 complex preferentially bound to two types of branched DNA substrates, the Y-shaped DNA and the synthetic Holliday junction, with almost equal affinities. A previous report showed that the BCDX2 complex binds to nicked linear dsDNA more strongly than linear dsDNA (30). Actually, the BCDX2 complex prepared in our studies also preferred the nicked duplex DNA prepared from oligonucleotides over the double-stranded oligonucleotide (data not shown). When the affinities towards the Y-shaped DNA and the nicked duplex DNA were compared, the BCDX2 complex showed a much stronger preference for the Y-shaped DNA. Furthermore, the BCDX2 complex preferred the Y-shaped DNA over the 5′- and 3′-tailed duplexes, in spite of the structural similarities of these substrates. These results suggest that the BCDX2 complex preferentially binds to the branch point of the Y-shaped DNA, since the other parts of the Y-shaped structure are the same as the tailed duplexes. The BCDX2 complex may move the branch of the Y-shaped DNA by its strand-annealing activity.

Strand annealing is an important reaction in HRR, and is essential for various HRR pathways, such as synthesis-dependent strand-annealing and single-strand annealing (57–59). Rad52 is a candidate for catalyzing the strand-annealing

reaction in HRR (54–56). In the present study, we have shown that the BCDX2 complex promotes strand annealing, with an activity comparable to that of Rad52. Therefore, the BCDX2 complex and Rad52 may have overlapping roles in the strand-annealing reaction of HRR. This is consistent with a previous genetic study, which suggested the redundant roles between the Rad51 paralogs and Rad52 in HRR (60).

The present study has revealed another important activity of the BCDX2 complex. Its binding affinity to the synthetic Holliday junction was significantly higher than that of the Rad51B protein. Recently, it was shown that Rad51C is required for Holliday-junction processing in mammalian cells (43). Moreover, the Rad51D·Xrcc2 sub-complex reportedly stimulates Holliday junction disruption by the BLM helicase (61). These observations suggest that, in addition to strand annealing, the BCDX2 complex may also be involved in Holliday junction processing in the late stages of HRR. The BCDX2 complex may be a multi-functional enzyme in HRR.

The strand-annealing reaction and the formation of branched DNA strands are not events restricted to recombination. These events probably occur in various other reactions of DNA metabolism, including DNA replication and gene transcription. For example, the Y-shaped DNA is found at the replication fork and at the transcribed sites of genes on chromosomes. The formation of a Holliday junction intermediate has been proposed in the repair of replication fork damage (58). Xrcc2 and Xrcc3 are both involved in replication fork progression (62). Therefore, the BCDX2 complex may be related to these processes. Further studies are required to understand these broad functional spectra of the BCDX2 complex in DNA metabolism.

ACKNOWLEDGEMENTS

We thank Takashi Kinebuchi (RIKEN GSC) for valuable discussions and technical assistance. This work was supported in part by the RIKEN Structural Genomics/Proteomics Initiative (RSGI), the National Project on Protein Structural and Functional Analyses, Grants-in-Aid from the Ministry of Education, Sports, Culture, Science and Technology, Japan, and from the Japanese Society for the Promotion of Science (JSPS), and also by the Bioarchitect Research Program (RIKEN) and CREST of JST (Japan Science and Technology).

REFERENCES

1. Whitaker,S.J. (1992) DNA damage by drugs and radiation: what is important and how is it measured? *Eur. J. Cancer*, **28**, 273–276.
2. Cox,M.M., Goodman,M.F., Kreuzer,K.N., Sherratt,D.J., Sandler,S.J. and Marians,K.J. (2000) The importance of repairing stalled replication forks. *Nature*, **404**, 37–41.
3. Ward,J.F. (1994) The complexity of DNA damage: relevance to biological consequences. *Int. J. Radiat. Biol.*, **66**, 427–432.
4. Caldecott,K.W. (2001) Mammalian DNA single-strand break repair: an X-ra(y)ted affair. *Bioessays*, **23**, 447–455.
5. van den Bosch,M., Lohman,P.H. and Pastink,A. (2002) DNA double-strand break repair by homologous recombination. *Biol. Chem.*, **383**, 873–892.
6. Shibata,T., DasGupta,C., Cunningham,R.P. and Radding,C.M. (1979) Purified *Escherichia coli* recA protein catalyzes homologous pairing of superhelical DNA and single-stranded fragments. *Proc. Natl Acad. Sci. USA*, **76**, 1638–1642.
7. McEntee,K., Weinstock,G.M. and Lehman,I.R. (1979) Initiation of general recombination catalyzed *in vitro* by the recA protein of *Escherichia coli*. *Proc. Natl Acad. Sci. USA*, **76**, 2615–2619.
8. West,S.C., Cassuto,E. and Howard-Flanders,P. (1981) recA protein promotes homologous-pairing and strand-exchange reactions between duplex DNA molecules. *Proc. Natl Acad. Sci. USA*, **78**, 2100–2104.
9. Cox,M.M. and Lehman,I.R. (1982) recA protein-promoted DNA strand exchange. Stable complexes of recA protein and single-stranded DNA formed in the presence of ATP and single-stranded DNA binding protein. *J. Biol. Chem.*, **257**, 8523–8532.
10. Shinohara,A., Ogawa,H., Matsuda,Y., Ushio,N., Ikeo,K. and Ogawa,T. (1993) Cloning of human, mouse and fission yeast recombination genes homologous to RAD51 and recA. *Nature Genet.*, **4**, 239–243.
11. Shinohara,A., Ogawa,H. and Ogawa,T. (1992) Rad51 protein involved in repair and recombination in *S.cerevisiae* is a RecA-like protein. *Cell*, **69**, 457–470.
12. Sung,P. (1994) Catalysis of ATP-dependent homologous DNA pairing and strand exchange by yeast RAD51 protein. *Science*, **265**, 1241–1243.
13. Baumann,P., Benson,F.E. and West,S.C. (1996) Human Rad51 protein promotes ATP-dependent homologous pairing and strand transfer reactions *in vitro*. *Cell*, **87**, 757–766.
14. Gupta,R.C., Bazemore,L.R., Golub,E.I. and Radding,C.M. (1997) Activities of human recombination protein Rad51. *Proc. Natl Acad. Sci. USA*, **94**, 463–468.
15. Albala,J.S., Thelen,M.P., Prange,C., Fan,W., Christensen,M., Thompson,L.H. and Lennon,G.G. (1997) Identification of a novel human RAD51 homolog, RAD51B. *Genomics*, **46**, 476–479.
16. Rice,M.C., Smith,S.T., Bullrich,F., Havre,P. and Kmiec,E.B. (1997) Isolation of human and mouse genes based on homology to REC2, a recombinational repair gene from the fungus *Ustilago maydis*. *Proc. Natl Acad. Sci. USA*, **94**, 7417–7422.
17. Cartwright,R., Dunn,A.M., Simpson,P.J., Tambini,C.E. and Thacker,J. (1998) Isolation of novel human and mouse genes of the recA/RAD51 recombination-repair gene family. *Nucleic Acids Res.*, **26**, 1653–1659.
18. Dosanjh,M.K., Collins,D.W., Fan,W., Lennon,G.G., Albala,J.S., Shen,Z. and Schild,D. (1998) Isolation and characterization of RAD51C, a new human member of the RAD51 family of related genes. *Nucleic Acids Res.*, **26**, 1179–1184.
19. Pittman,D.L., Weinberg,L.R. and Schimenti,J.C. (1998) Identification, characterization and genetic mapping of Rad51d, a new mouse and human RAD51/RecA-related gene. *Genomics*, **49**, 103–111.
20. Cartwright,R., Tambini,C.E., Simpson,P.J. and Thacker,J. (1998) The XRCC2 DNA repair gene from human and mouse encodes a novel member of the recA/RAD51 family. *Nucleic Acids Res.*, **26**, 3084–3089.
21. Liu,N., Lamerdin,J.E., Tebbs,R.S., Schild,D., Tucker,J.D., Shen,M.R., Brookman,K.W., Siciliano,M.J., Walter,C.A., Fan,W. *et al.* (1998) XRCC2 and XRCC3, new human Rad51-family members, promote chromosome stability and protect against DNA cross-links and other damages. *Mol. Cell*, **1**, 783–793.
22. Tebbs,R.S., Zhao,Y., Tucker,J.D., Scheerer,J.B., Siciliano,M.J., Hwang,M., Liu,N., Legerski,R.J. and Thompson,L.H. (1995) Correction of chromosomal instability and sensitivity to diverse mutagens by a cloned cDNA of the XRCC3 DNA repair gene. *Proc. Natl Acad. Sci. USA*, **92**, 6354–6358.
23. Johnson,R.D., Liu,N. and Jasin,M. (1999) Mammalian XRCC2 promotes the repair of DNA double-strand breaks by homologous recombination. *Nature*, **401**, 397–399.
24. Pierce,A.J., Johnson,R.D., Thompson,L.H. and Jasin,M. (1999) XRCC3 promotes homology-directed repair of DNA damage in mammalian cells. *Genes Dev.*, **13**, 2633–2638.
25. Takata,M., Sasaki,M.S., Sonoda,E., Fukushima,T., Morrison,C., Albala,J.S., Swagemakers,S.M., Kanaar,R., Thompson,L.H. and Takeda,S. (2000) The Rad51 paralog Rad51B promotes homologous recombinational repair. *Mol. Cell. Biol.*, **20**, 6476–6482.
26. Takata,M., Sasaki,M.S., Tachiiri,S., Fukushima,T., Sonoda,E., Schild,D., Thompson,L.H. and Takeda,S. (2001) Chromosome instability and defective recombinational repair in knockout mutants of the five Rad51 paralogs. *Mol. Cell. Biol.*, **21**, 2858–2866.
27. Godthelp,B.C., Wiegant,W.W., van Duijn-Goedhart,A., Scharer,O.D., van Buul,P.P., Kanaar,R. and Zdzienicka,M.Z. (2002) Mammalian Rad51C contributes to DNA cross-link resistance, sister chromatid cohesion and genomic stability. *Nucleic Acids Res.*, **30**, 2172–2182.
28. Bishop,D.K., Ear,U., Bhattacharyya,A., Calderone,C., Beckett,M., Weichselbaum,R.R. and Shinohara,A. (1998) Xrcc3 is required for

assembly of Rad51 complexes *in vivo*. *J. Biol. Chem.*, **273**, 21482–21488.
29. Kurumizaka,H., Ikawa,S., Nakada,M., Eda,K., Kagawa,W., Takata,M., Takeda,S., Yokoyama,S. and Shibata,T. (2001) Homologous-pairing activity of the human DNA-repair proteins Xrcc3.Rad51C. *Proc. Natl Acad. Sci. USA*, **98**, 5538–5543.
30. Masson,J.Y., Tarsounas,M.C., Stasiak,A.Z., Stasiak,A., Shah,R., McIlwraith,M.J., Benson,F.E. and West,S.C. (2001) Identification and purification of two distinct complexes containing the five RAD51 paralogs. *Genes Dev.*, **15**, 3296–3307.
31. Wiese,C., Collins,D.W., Albala,J.S., Thompson,L.H., Kronenberg,A. and Schild,D. (2002) Interactions involving the Rad51 paralogs Rad51C and XRCC3 in human cells. *Nucleic Acids Res.*, **30**, 1001–1008.
32. Liu,N., Schild,D., Thelen,M.P. and Thompson,L.H. (2002) Involvement of Rad51C in two distinct protein complexes of Rad51 paralogs in human cells. *Nucleic Acids Res.*, **30**, 1009–1015.
33. Miller,K.A., Yoshikawa,D.M., McConnell,I.R., Clark,R., Schild,D. and Albala,J.S. (2002) RAD51C interacts with RAD51B and is central to a larger protein complex *in vivo* exclusive of RAD51. *J. Biol. Chem.*, **277**, 8406–8411.
34. Masson,J.Y., Stasiak,A.Z., Stasiak,A., Benson,F.E. and West,S.C. (2001) Complex formation by the human RAD51C and XRCC3 recombination repair proteins. *Proc. Natl Acad. Sci. USA*, **98**, 8440–8446.
35. Kurumizaka,H., Enomoto,R., Nakada,M., Eda,K., Yokoyama,S. and Shibata,T. (2003) Region and amino acid residues required for Rad51C binding in the human Xrcc3 protein. *Nucleic Acids Res.*, **31**, 4041–4050.
36. Miller,K.A., Sawicka,D., Barsky,D. and Albala,J.S. (2004) Domain mapping of the Rad51 paralog protein complexes. *Nucleic Acids Res.*, **32**, 169–178.
37. Schild,D., Lio,Y.C., Collins,D.W., Tsomondo,T. and Chen,D.J. (2000) Evidence for simultaneous protein interactions between human Rad51 paralogs. *J. Biol. Chem.*, **275**, 16443–16449.
38. Lio,Y.C., Mazin,A.V., Kowalczykowski,S.C. and Chen,D.J. (2003) Complex formation by the human Rad51B and Rad51C DNA repair proteins and their activities *in vitro*. *J. Biol. Chem.*, **278**, 2469–2478.
39. Kurumizaka,H., Ikawa,S., Nakada,M., Enomoto,R., Kagawa,W., Kinebuchi,T., Yamazoe,M., Yokoyama,S. and Shibata,T. (2002) Homologous pairing and ring and filament structure formation activities of the human Xrcc2·Rad51D complex. *J. Biol. Chem.*, **277**, 14315–14320.
40. Sigurdsson,S., Van Komen,S., Bussen,W., Schild,D., Albala,J.S. and Sung,P. (2001) Mediator function of the human Rad51B-Rad51C complex in Rad51/RPA-catalyzed DNA strand exchange. *Genes Dev.*, **15**, 3308–3318.
41. Braybrooke,J.P., Spink,K.G., Thacker,J. and Hickson,I.D. (2000) The RAD51 family member, RAD51L3, is a DNA-stimulated ATPase that forms a complex with XRCC2. *J. Biol. Chem.*, **275**, 29100–29106.
42. Yokoyama,H., Kurumizaka,H., Ikawa,S., Yokoyama,S. and Shibata,T. (2003) Holliday junction binding activity of the human Rad51B protein. *J. Biol. Chem.*, **278**, 2767–2772.
43. Liu,Y., Masson,J.Y., Shah,R., O'Regan,P. and West,S.C. (2004) RAD51C is required for Holliday junction processing in mammalian cells. *Science*, **303**, 243–246.
44. Kurumizaka,H., Aihara,H., Kagawa,W., Shibata,T. and Yokoyama,S. (1999) Human Rad51 amino acid residues required for Rad52 binding. *J. Mol. Biol.*, **291**, 537–548.
45. Kagawa,W., Kurumizaka,H., Ikawa,S., Yokoyama,S. and Shibata,T. (2001) Homologous pairing promoted by the human Rad52 protein. *J. Biol. Chem.*, **276**, 35201–35208.
46. Kurumizaka,H., Aihara,H., Ikawa,S. and Shibata,T. (2000) Specific defects in double-stranded DNA unwinding and homologous pairing of a mutant RecA protein. *FEBS Lett.*, **477**, 129–134.
47. Tombline,G. and Fishel,R. (2002) Biochemical characterization of the human RAD51 protein. I. ATP hydrolysis. *J. Biol. Chem.*, **277**, 14417–14425.
48. Roca,A.I. and Cox,M.M. (1990) The RecA protein: structure and function. *Crit. Rev. Biochem. Mol. Biol.*, **25**, 415–456.
49. Cox,M.M. (1994) Why does RecA protein hydrolyse ATP? *Trends Biochem. Sci.*, **19**, 217–222.
50. Hortnagel,K., Voloshin,O.N., Kinal,H.H., Ma,N., Schaffer-Judge,C. and Camerini-Otero,R.D. (1999) Saturation mutagenesis of the *E. coli* RecA loop L2 homologous DNA pairing region reveals residues essential for recombination and recombinational repair. *J. Mol. Biol.*, **286**, 1097–1106.
51. Voloshin,O.N., Wang,L. and Camerini-Otero,R.D. (2000) The homologous pairing domain of RecA also mediates the allosteric regulation of DNA binding and ATP hydrolysis: a remarkable concentration of functional residues. *J. Mol. Biol.*, **303**, 709–720.
52. McGrew,D.A. and Knight,K.L. (2003) Molecular design and functional organization of the RecA protein. *Crit. Rev. Biochem. Mol. Biol.*, **38**, 385–432.
53. Cox,M.M. (2003) The bacterial RecA protein as a motor protein. *Annu. Rev. Microbiol.*, **57**, 551–577.
54. Mortensen,U.H., Bendixen,C., Sunjevaric,I. and Rothstein,R. (1996) DNA strand annealing is promoted by the yeast Rad52 protein. *Proc. Natl Acad. Sci. USA*, **93**, 10729–10734.
55. Reddy,G., Golub,E.I. and Radding,C.M. (1997) Human Rad52 protein promotes single-strand DNA annealing followed by branch migration. *Mutat. Res.*, **377**, 53–59.
56. Sugiyama,T., New,J.H. and Kowalczykowski,S.C. (1998) DNA annealing by RAD52 protein is stimulated by specific interaction with the complex of replication protein A and single-stranded DNA. *Proc. Natl Acad. Sci. USA*, **95**, 6049–6054.
57. Paques,F. and Haber,J.E. (1999) Multiple pathways of recombination induced by double-strand breaks in *Saccharomyces cerevisiae*. *Microbiol. Mol. Biol. Rev.*, **63**, 349–404.
58. Cromie,G.A., Connelly,J.C. and Leach,D.R. (2001) Recombination at double-strand breaks and DNA ends: conserved mechanisms from phage to humans. *Mol. Cell*, **8**, 1163–1174.
59. Prado,F., Cortes-Ledesma,F., Huertas,P. and Aguilera,A. (2003) Mitotic recombination in *Saccharomyces cerevisiae*. *Curr. Genet.*, **42**, 185–198.
60. Fujimori,A., Tachiiri,S., Sonoda,E., Thompson,L.H., Dhar,P.K., Hiraoka,M., Takeda,S., Zhang,Y., Reth,M. and Takata,M. (2001) Rad52 partially substitutes for the Rad51 paralog XRCC3 in maintaining chromosomal integrity in vertebrate cells. *EMBO J.*, **20**, 5513–5520.
61. Braybrooke,J.P., Li,J.L., Wu,L., Caple,F., Benson,F.E. and Hickson,I.D. (2003) Functional interaction between the Bloom's syndrome helicase and the RAD51 paralog, RAD51L3 (RAD51D). *J. Biol. Chem.*, **278**, 48357–48366.
62. Henry-Mowatt,J., Jackson,D., Masson,J.Y., Johnson,P.A., Clements,P.M., Benson,F.E., Thompson,L.H., Takeda,S., West,S.C. and Caldecott,K.W. (2003) XRCC3 and Rad51 modulate replication fork progression on damaged vertebrate chromosomes. *Mol. Cell*, **11**, 1109–1117.